Supercharged Homogeneous Charge Compression Ignition

Christensen, Magnus; Johansson, Bengt; Amnéus, Per; Mauss, Fabian

Published in:
SAE Transactions, Journal of Engines

1998

SAE TECHNICAL PAPER SERIES

980787

Supercharged Homogeneous Charge Compression Ignition

Magnus Christensen and Bengt Johansson
Division of Combustion Engines, Lund Institute of Technology

Per Amnéus and Fabian Mauss
Division of Combustion Physics, Lund Institute of Technology

Reprinted From: Combustion Processes in Diesel Engines (SP-1328)

SAE The Engineering Society For Advancing Mobility Land Sea Air and Space® INTERNATIONAL

International Congress and Exposition
Detroit, Michigan
February 23-26, 1998

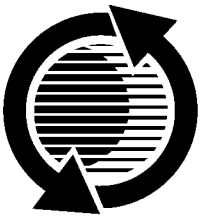

ISSN 0148-7191

Printed in USA

980787

Supercharged Homogeneous Charge Compression Ignition

Magnus Christensen and Bengt Johansson
Division of Combustion Engines, Lund Institute of Technology

Per Amnéus and Fabian Mauss
Division of Combustion Physics, Lund Institute of Technology

ABSTRACT

The Homogeneous Charge Compression Ignition (HCCI) is the third alternative for combustion in the reciprocating engine. Here, a homogeneous charge is used as in a spark ignited engine, but the charge is compressed to auto-ignition as in a diesel. The main difference compared with the Spark Ignition (SI) engine is the lack of flame propagation and hence the independence from turbulence. Compared with the diesel engine, HCCI has a homogeneous charge and hence no problems associated with soot and NO_X formation. Earlier research on HCCI showed high efficiency and very low amounts of NO_X, but HC and CO were higher than in SI mode. It was not possible to achieve high IMEP values with HCCI, the limit being 5 bar. Supercharging is one way to dramatically increase IMEP. The influence of supercharging on HCCI was therefore experimentally investigated. Three different fuels were used during the experiments: *iso*-octane, ethanol and natural gas. Two different compression ratios were used, 17:1 and 19:1. The inlet pressure conditions were set to give 0, 1 or 2 bar of boost pressure. The highest attainable IMEP was 14 bar using natural gas as fuel at the lower compression ratio. The limit in achieving even higher IMEP was set by the high rate of combustion and a high peak pressure.

Numerical calculations of the HCCI process have been performed for natural gas as fuel. The calculated ignition timings agreed well with the experimental findings. The numerical solution, is however, very sensitive to the composition of the natural gas.

INTRODUCTION

The Homogeneous Charge Compression Ignition, HCCI, the concept is a hybrid of the successful Spark Ignition (SI) and Compression Ignition (CI) engine concepts. As in a diesel engine, the fuel is exposed to a sufficiently high temperature for auto ignition to occur, but in HCCI, a homogeneous fuel/air mixture is used. The homogeneous mixture is created in the intake system, as in an SI engine, using a low-pressure injection system or a carburetor. No ignition system is necessary. To limit the rate of combustion, very diluted mixtures must be used. This high dilution can be achieved by a high air/fuel ratio and/or with Exhaust Gas Recycling (EGR). If the mixture is too rich, the rate of combustion becomes too rapid and will generate knock-related problems.

A too lean mixture will lead to incomplete combustion or misfire. In SI engines, large cycle-to-cycle variations occur since the early flame development varies considerably due to mixture inhomogeneities in the vicinity of the spark plug [1]. With HCCI, cycle-to-cycle variations of combustion are very small, since combustion initiation takes place at many points at the same time. The whole mixture burns almost homogeneously. In this way, unstable flame propagation is avoided.

PREVIOUS WORK – The first studies on HCCI were performed on a two stroke engine by Onishi et al. in 1979. They called it Active-Thermo Atmosphere Combustion (ATAC) [2]. They showed that there is no flame propagation, as in a conventional SI engine. Instead, the whole mixture burns slowly at the same time. Not long after the presentation of Onishi et al., Noguchi et al. demonstrated the same combustion process in an opposed-piston two stroke engine [3]. They also conducted measurements of radical concentration during combustion. In 1994, Iida showed that the possible operating conditions for stable two-stroke HCCI combustion could be significantly broadened by using methanol as fuel [4]., Honda has recently demonstrated a concept for HCCI combustion for a production two stroke engine [5] and proved the reliability of the concept by competing in the Granada-Dakar desert race with a pre-production motorcycle [6]. A pre-production two-stroke engine deploying HCCI has also been shown by IFP [7]. In both cases, HCCI was used to improve part load combustion stability, reduce HC emissions and improve fuel economy at part load.

In 1983 Njat and Foster showed that it was also possible to achieve HCCI in a four stroke engine [8]. They used an engine with variable compression operating on a mixture of *iso*-octane and n-heptane.

The first to suggest the use of conventional SI operation at high loads and HCCI at part loads was Thring [9]. He used both gasoline and diesel fuel, and investigated possible combinations of λ and EGR. This work was later continued by Ryan and Callahan, who found that a low compression ratio was necessary when using diesel fuel [10], otherwise, auto-ignition occurred to early during the compression stroke.

The first to test HCCI on an real production engine was Stockinger et al. in 1992 [11]. They used a standard 1.6 litre VW engine which was converted to HCCI operation with preheated intake air. The part load efficiency increased from 14 to 34%.

Our own earlier research on HCCI showed that the indicated efficiency was much higher with HCCI than with SI operation at part load [12]. Very little NO_X was generated with HCCI, but HCCI generated about twice the amout of HC. The amount of CO generated depended much on the air/fuel ratio. Close to the rich limit, very little CO was generated. The low IMEP attainable with HCCI was noted as a limit for future commercial use of the HCCI concept.

Interesting research on HCCI has been carried out by Aoyama et al. [13]. They made comparisons between HCCI, diesel and Gasoline Direct Injection (GDI) operation. At the optimum value of λ, HCCI exhibited the lowest fuel consumption and a much lower emission of NO_X but HC emissions were higher. They also used supercharging to increase the engine output. However, the boost pressure used in this study was rather low, and no conclusions could be drawn regarding the possibility of reaching an engine torque comparable to that in SI operation.

In summary, previous studies on HCCI have shown that it can be used in both two-stroke and four-stroke engines. The practical operating conditions are, however, limited due to the requirements on combustion rate. In two-stroke engines, this results in a requirement of high residual gas concentration, which is found at part load. In four-stroke engines, which normally have much less residual gas, ultra-lean mixtures or large amounts of EGR must be used. The emission of NO_X has been reported to be very low, in most cases only a few ppm.

PRESENT WORK – The low IMEP achieved with naturally aspirated HCCI limits future commercial use of the HCCI concept. To clarify the effect of supercharging on HCCI, especially on the HC emissions and on the upper load limit, a serie of tests was carried out. Boost pressures up to 2 bar were used. The boost pressure was generated by an external air compressor. It was decided to use a four-stroke engine operating at low engine speed. The engine speed was set to 1000 rpm during all experiments. Three fuels were used during the experiments: *iso*-octane was selected to serve as a reference fuel, ethanol is of interest as a future replacement for gasoline and natural gas is also of interest as an alternative fuel and was interesting since it is a gaseous fuel and hence has no heat of vaporization. The octane number of the three fuels are 100, 106 and 120, respectively. Two different compression ratios were used, 17:1 and 19:1.

As the HCCI combustion process is controlled by chemistry only, simulation of the process using chemical kinetics can be fruitful. Therefore combustion in the experiments with natural gas as fuel were simulated using a kinetic mechanism containing 65 species and 700 reactions.

EXPERIMENTAL APPARATUS

THE ENGINE – A diesel engine was converted to run in HCCI mode. The engine was originally a Volvo TD100 series diesel. The in-line six cylinder engine was, however, modified to operate on one cylinder only. This arrangement gives a robust and inexpensive single-cylinder engine, but at the cost of the reliability of the brake specific results. With a pressure transducer, indicated results can be used instead. The most important engine parameters are shown in table 1. Futher details on the engine can be found in [14].

Table 1. Geometric properties of the engine.

Displaced Volume	*1600 cm^3*
Bore	*120.65 mm*
Stroke	*140 mm*
Connection Rod	*260 mm*
Exhaust Valve Open	*39° BBDC (at 1 mm lift)*
Exhaust Valve Close	*10° BTDC (at 1 mm lift)*
Inlet Valve Open	*5° ATDC (at 1 mm lift)*
Inlet Valve Close	*13° ABDC (at 1 mm lift)*

To initiate HCCI combustion, high temperature and pressure are necessary. HCCI is not dependent on turbulence for flame propagation or swirling flow for diffusion combustion. In consequence, the simplest possible combustion chamber geometry was selected, a flat piston crown giving a pancake combustion chamber. The piston with the lower compression ratio was slightly chamfered, to investigate if this had any influence on the HC emission. The inlet air was preheated with an electrical heater during the experiments.

FUEL – The gas fuel used was common commercially available natural gas. This means that its predominate compound is methane, with a non-negligible content of other gases, mainly higher hydrocarbons. The other fuels used were *iso*-octane and ethanol.

Table 2. Composition of the natural gas used.

Component	*Vol. %*	*Mass %*
Methane	*91.1*	*81.0*
Ethane	*4.7*	*7.9*
Propane	*1.7*	*4.2*
n-Butane	*1.4*	*4.7*
Nitrogen	*0.6*	*0.9*
Carbon dioxide	*0.5*	*1.2*

RESULTS

AIR/FUEL EQUIVALENCE RATIO, λ – Figures 1-3 show the values of λ used. λ is the ratio of the actual air/fuel ratio to the stoichiometric air/fuel ratio. The values of lambda are calculated from the exhaust gas composition. It should be noted that when using natural gas a richer mixture was used than when ethanol or *iso*-octane were used.

INLET AIR TEMPERATURE – With HCCI, the inlet air must be preheated. The degree of preheating depends on the compression ratio, the fuel (heat of vaporization and octane number) and λ. The legends in figures 1-3 give the inlet temperatures used to achieve HCCI combustion close to top dead centre (TDC) for the operating conditions used. The required preheating is greatly reduced by an increase in inlet pressure. With two bar supercharging pressure the preheating requirement is lower than the temperature increase resulting from compression in a supercharger. This means that no extra equipment would be needed for preheating. In naturally aspirated (NA) operation, with 1 bar boost pressure, the inlet temperature must be higher for natural gas. This is expected from the higher octane number. However, with 2 bar supercharging, natural gas requires less preheating than ethanol. This indicates a higher pressure sensitivity for methane auto-ignition compared with ethanol, and *iso*-octane is even less sensitive.

ENGINE LOAD, IMEP – one major limitation of HCCI combustion is the requirement of a highly diluted mixture in order to slow down the speed of the chemical reactions sufficiently, for reasonably slow combustion. The mixture can be diluted with air or/and with EGR. In this study, air was used. With lean operation, this will significantly reduce the output power for a given air flow through the engine. The air flow can, however, be increased by supercharging. Three different levels of inlet pressure were used in the experiments presented. First, the engine was operated NA, and then a boost pressure of 1 and 2 bar was used, giving 1, 2 and 3 bar of absolute pressure for the three cases. Most results presented are as a function of Indicated Mean Effective Pressure, IMEP. It is evaluated over all four engine stokes and is thus IME-P_{net}.

The rich side limit for IMEP is set by combustion rate and hence rate of pressure rise. As shown later, the maximum pressure rise rate was set to 12 bar per Crank Angle Degree (CAD) for the naturally aspirated case, and approximately 20 bar/CAD for the supercharged cases. A limitation in maximum pressure of 250 bar was also chosen to prevent excessive mechanical stress in the engine structure.

To serve as a reference, the same measurements were performed without supercharging (0 bar boost pressure) as for the supercharged cases. Figure 1 shows that *iso*-octane gives the highest usable IMEP without supercharging using a compression ratio of 17:1. However, *iso*-octane could not used with the higher compression ratio, 19:1, due to much too early combustion initiation. For ethanol and natural gas, the attainable IMEP was higher for the lower compression ratio. This is expected, as combustion initiation takes place later with a lower compression ratio.

Figures 2 and 3 show a decrease in IMEP for *iso*-octane with supercharging compared with the other fuels. This is the result of an earlier combustion and hence higher maximum pressure and pressure rise rate. *Iso*-octane exhibits more knocking-like combustion than ethanol and natural gas, when supercharging is employed. Ethanol shows a linear relation between IMEP and inlet pressure for all three inlet pressures. Natural gas at the lower compression ratio gave the highest IMEP, with both one and two bar of supercharging pressure. The much lower IMEP for one bar supercharging using the higher compression ratio is due to the leaner operation.

GROSS INDICATED EFFICIENCY – The gross indicated efficiency was evaluated by measuring the fuel flow and the indicated mean effective pressure during the compression and expansion strokes only. This means that the effect of supercharging on the gas exchange process is absent. Figures 4-6 show the gross indicated efficiency for the different cases.

Figure 4 shows a higher gross indicated efficiency for ethanol running at a 19:1 compression ratio than at 17:1. This is expected. The increase in efficiency of an ideal cycle with heat addition removal at constant volume is given by

$$\eta = 1 - \frac{1}{r_c^{\gamma-1}}$$

with γ = 1.4 and the compression ratio, r_c set to 17 or 19 we obtain the efficiencies to 0.678 and 0.692. The ratio between these is 1.02, whereas the ratio obtained from Figure 4 is 0.50/0.48 = 1.04. This means that the efficiency gain with ethanol is the result from not only the increase in compression ratio.

With increased inlet pressure the efficiency obtained with *iso*-octane is reduced, especially for the 2 bar case. This is the result of early combustion initiation, as shown in Figure 37. Ethanol shows an increased efficiency with supercharging. The runs at 17:1 and 19:1 compression

ratio show similar trends. Natural gas is influenced very little by the pressure level but shows a strange efficiency decrease with increased load, especially for the NA case.

COMBUSTION EFFICIENCY – The combustion efficiency was evaluated from the exhaust gas analysis (HC and CO). Figures 7-9 show the combustion efficiency. Figure 7 shows that the combustion efficiency increases with engine load. This is due to the use of a richer mixture and hence higher temperature. For the supercharged cases, Figure 8 and 9, this trend is less obvious. Pressure effects on combustion can play a larger role here. For all cases, the highest combustion efficiency is yielded with ethanol as fuel. Natural gas is better than *iso*-octane without supercharging but has a major drop at 1 or 2 bar inlet pressure. For both ethanol and natural gas, the combustion efficiency is increased with a higher compression ratio.

PUMPING MEAN EFFECTIVE PRESSURE – Figure 13-15 show the pumping mean effective pressure for the different cases. It can be noted that ethanol has a higher PMEP than the other two fuels. This is due to the lower exhaust gas temperature resulting from the higher gross indicated efficiency. The lower exhaust gas temperature gives less blow down at exhaust valve opening and hence more mass remains in the cylinder to be expelled by the upward motion of the piston during the exhaust stroke. The engine used is a converted diesel engine with a relatively small exhaust valve. The valve area is sufficient for diesel operation but causes a restriction of the larger flows associated with supercharging with a very lean mixture. A considerable pumping loss then results.

NET INDICATED EFFICIENCY – The net indicated efficiency is obtained from the fuel flow and the indicated mean effective pressure during all four strokes. The gas exchange process is thus included here. This means that the net indicated efficiency is lower than the gross indicated efficiency for the cases without supercharging. For the supercharged cases, the net indicated efficiency is higher than the gross indicated efficiency, due to the use of an external supercharging system. Figures 10-12 show the obtained net indicated efficiency. Ethanol gives the best result but natural gas has gained somewhat on its lower PMEP.

In a production engine the power required for supercharging would be taken from the engine itself, resulting in a lower efficiency. Some of this power loss, however, returns to the engine as a decrease in pumping work.

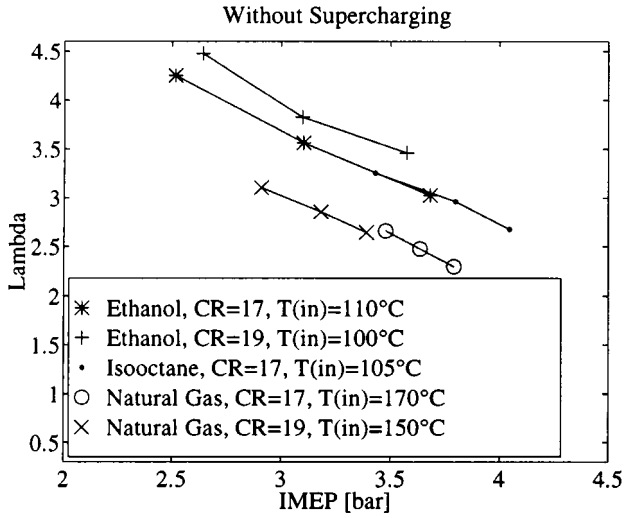

Figure 1. Lambda without supercharging.

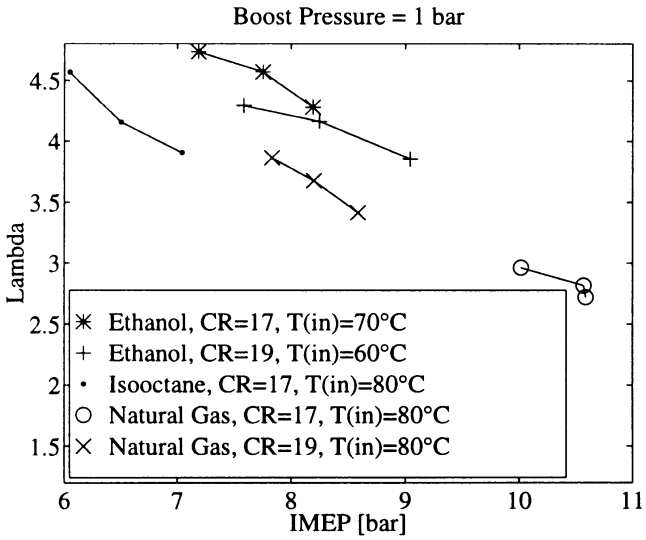

Figure 2. Lambda for 1 bar boost pressure.

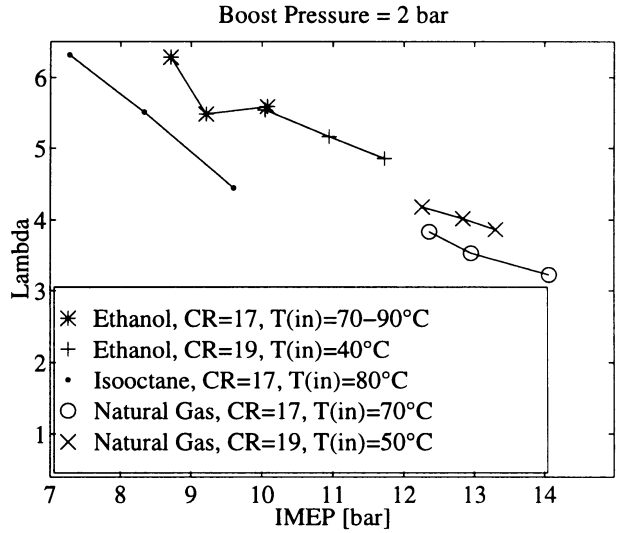

Figure 3. Lambda for 2 bar boost pressure.

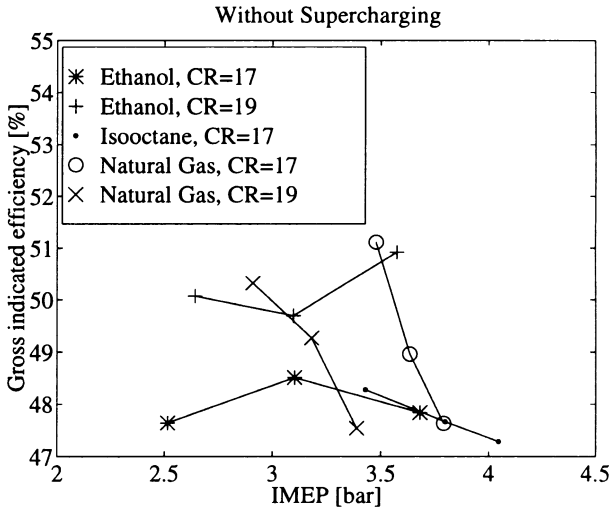

Figure 4. Gross indicated efficiency without supercharging.

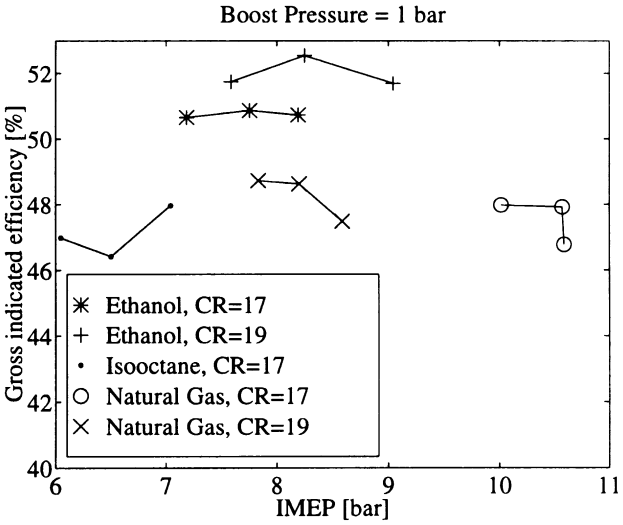

Figure 5. Gross indicated efficiency for 1 bar boost pressure.

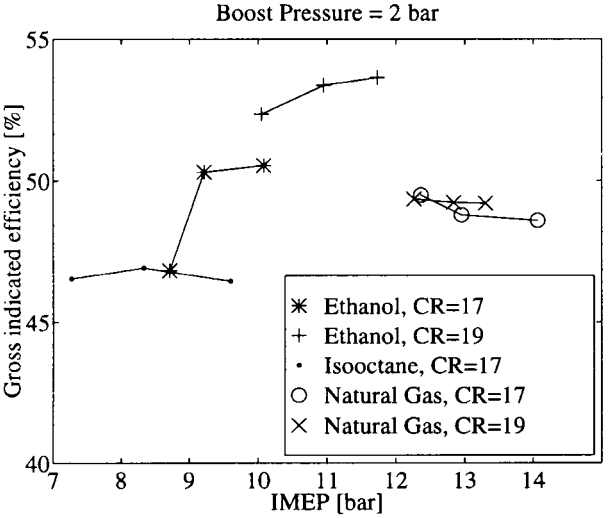

Figure 6. Gross indicated efficiency for 2 bar boost pressure.

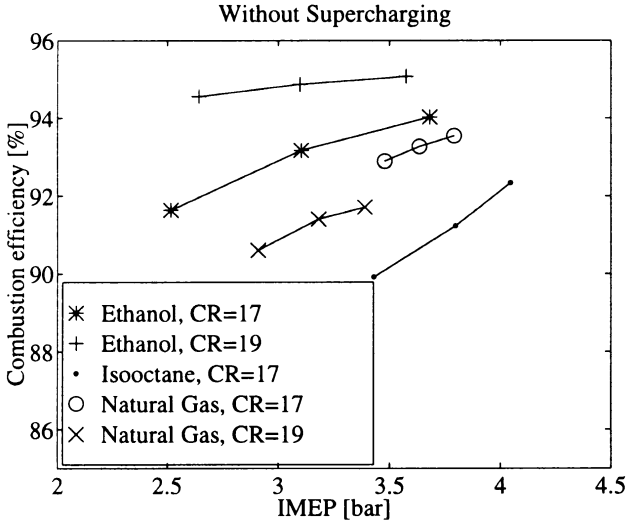

Figure 7. Combustion efficiency without supercharging.

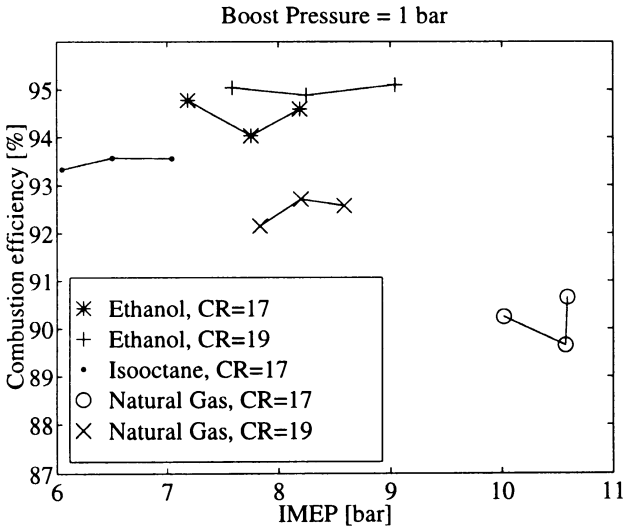

Figure 8. Combustion efficiency for 1 bar boost pressure.

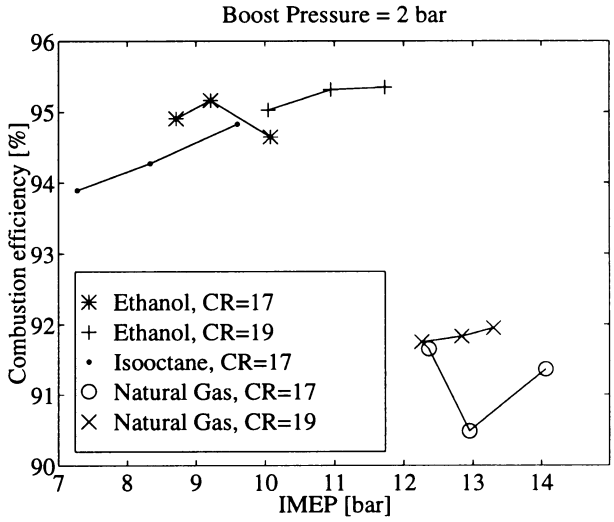

Figure 9. Combustion efficiency for 2 bar boost pressure.

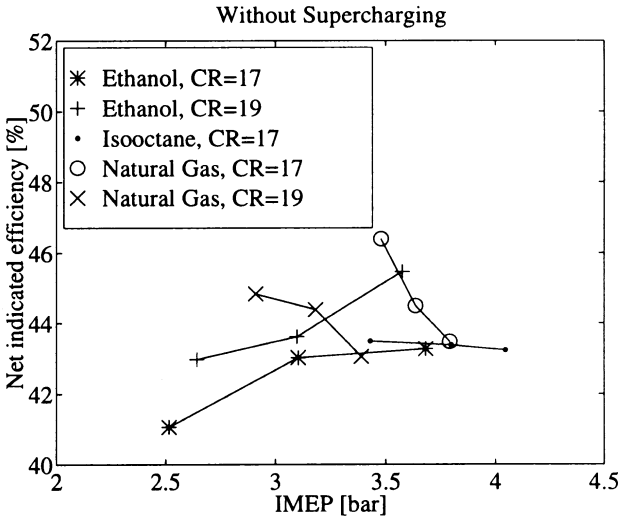

Figure 10. Net indicated efficiency without supercharging.

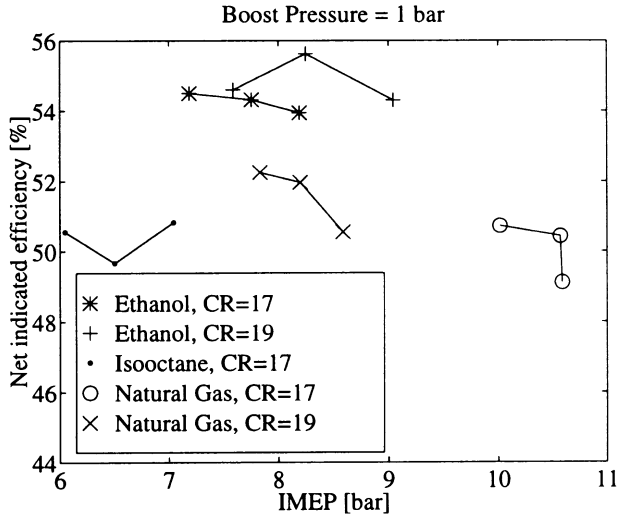

Figure 11. Net indicated efficiency for 1 bar boost pressure.

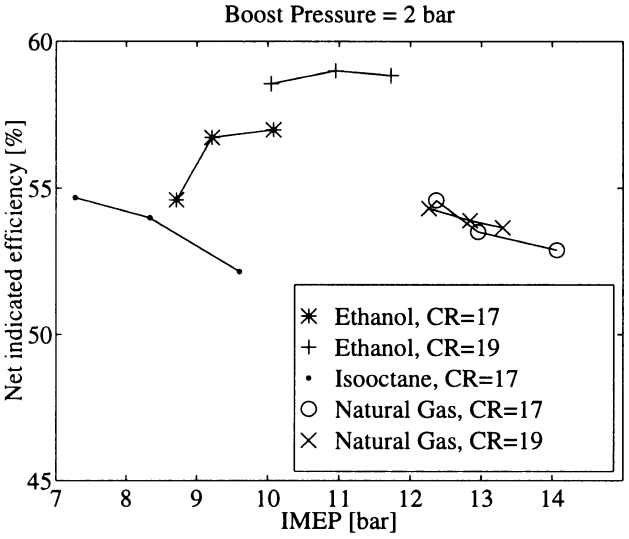

Figure 12. Net indicated efficiency for 2 bar boost pressure.

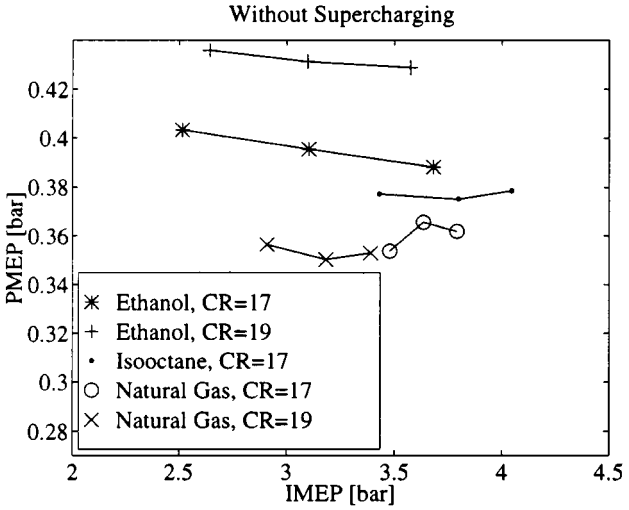

Figure 13. Pumping mean effective pressure without supercharging, running on iso-octane.

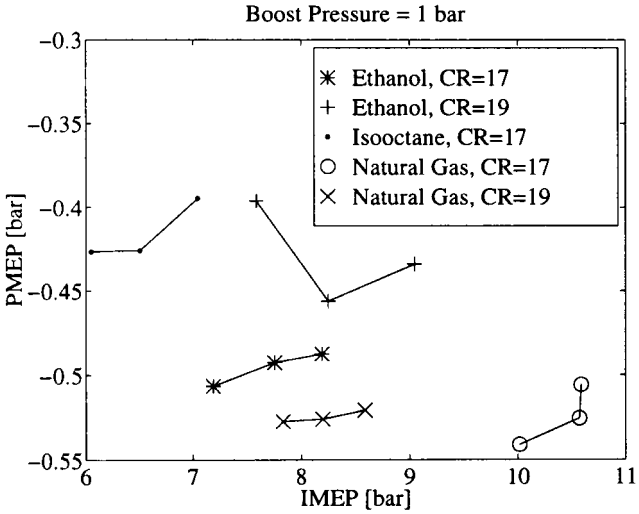

Figure 14. Pumping mean effective pressure for 1 bar boost pressure, running on iso-octane.

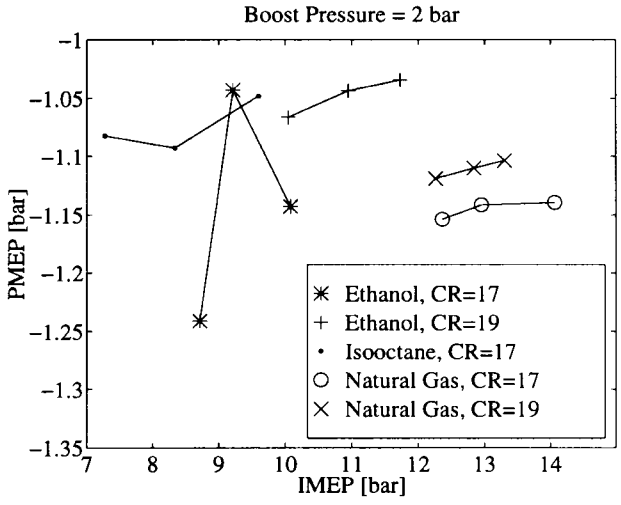

Figure 15. Pumping mean effective pressure for 2 bar boost pressure, running on iso-octane.

NO_X – One of the most appealing attributes of HCCI is the homogeneous combustion. This means that the temperature should be the same in the entire combustion chamber. This, in combination with the ultra lean mixtures required to control the combustion rate, gives a very low maximum temperature during the cycle. Figures 16-18 show the indicated specific NO_X emission. The levels are very low, as low as after a well functioning three-way catalyst or even better. The trend observable from Figures 16-18 is an increase in NO_X for the richest mixtures when running on *iso*-octane. This indicates that the maximum temperature during the cycle is approaching the limit of thermal NO_X production. It can also be noted that less NO_X is generated with a lower inlet temperature. This shows that the NO is temperature sensitive even below the thermal NO temperature limit. A consequence of this is lower NO_X in the supercharged cases. They require less preheat to burn at the correct crank angle position. The NO_X is one order of magnitude lower with two bar boost pressure than in the naturally aspirated case.

HC – Emissions of unburned hydrocarbons are generated in several ways. One of the major causes of HC in SI engines is fuel trapped in the crevice volume. Up to ten per cent of the fuel mass can escape into the crevice volume and not be included in the original combustion, and combustion must hence rely on post flame oxidization. The reason for this high value is that flame propagation usually takes place from a centrally located spark plug. The flame “pushes” unburned mixture down into the crevices during its progress. With HCCI, less fuel should be trapped in the crevices as there is no flame front. As the pressure in the cylinder rises, a large fraction of the gas that is pushed into the crevices has already burned and hence does not contribute to HC emissions. However, crevice effects are not the only mechanism for HC. There is also wall and bulk quenching. These mechanisms are not considered important in an engine operating under stoichiometric conditions, but with HCCI ultra lean mixtures are used. The relative importance of crevice effects and quenching is not known for such ultra lean mixtures. Figures 19-21 show the indicated specific HC emission. Figure 19 shows a decrease in HC with higher loads. This is expected as the temperature in the cylinder increases with engine load. Thus quenching distances will tend to decrease.

With an increase in inlet pressure, and hence IMEP, the specific emissions of HC are reduced for *iso*-octane and ethanol. Natural gas gives the lowest levels of HC when the engine is naturally aspirated. With higher boost pressures natural gas and ethanol produce comparable levels of HC.

An indication of the lesser importance of crevice effects on HC in HCCI operation is provided by the results from operation at different compression ratios. The pistons used for the two compression ratios are basically the same. The volume removed from the piston giving a compression ratio of 17:1 was located above the upper piston ring. Extending the distance between the piston and the cylinder (top land) is a well known method of reducing HC from SI engines [15]. But in this case the lower compression ratio gave increased HC in five out of six cases.

CO – Emission of carbon monoxide is generally an indication of incomplete oxidation of fuel (low air/fuel ratio). With HCCI, CO is very dependent on load and preheating. With high load and hot inlet air, little CO is generated. Figures 22-24 show the specific CO emissions.

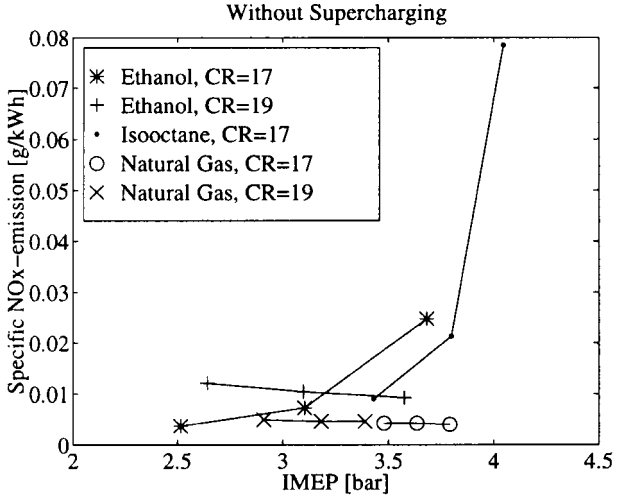

Figure 16. Specific NO_X emission without supercharging.

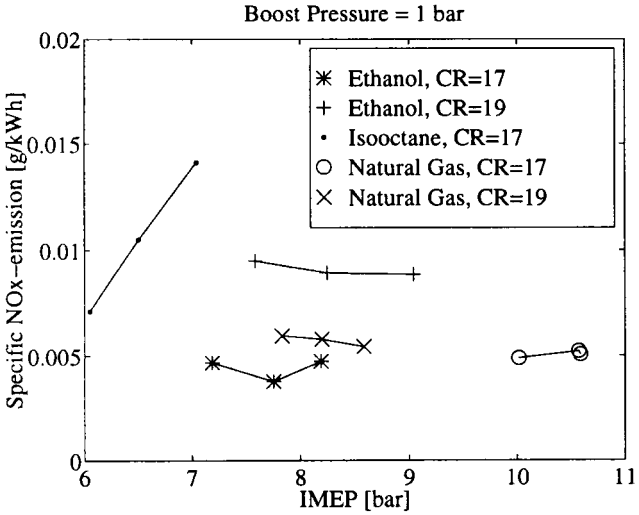

Figure 17. Specific NO_X emission, 1 bar boost pressure

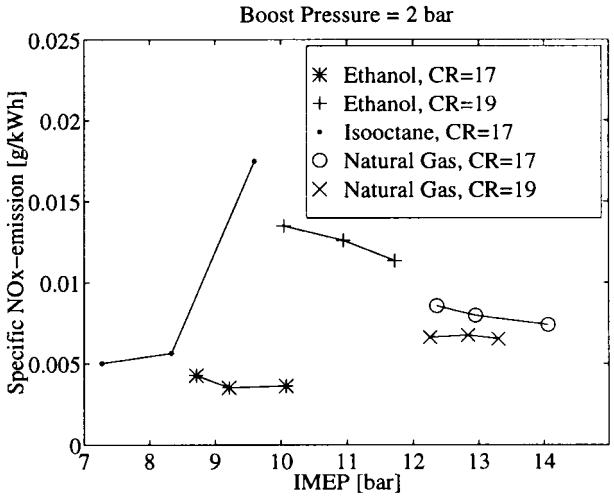

Figure 18. Specific NO_X emission, 2 bar boost pressure

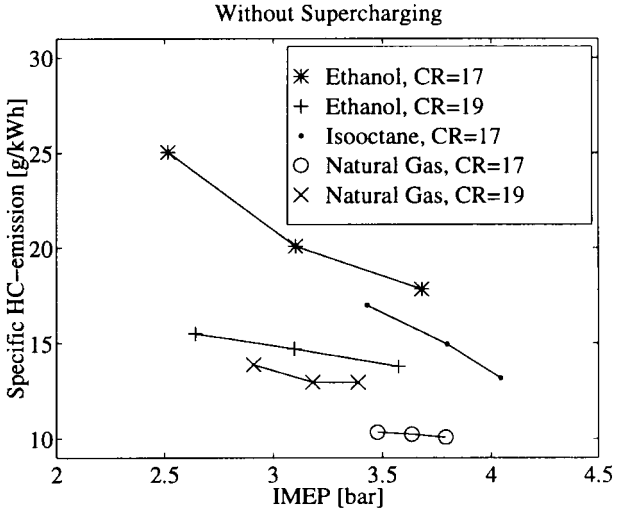

Figure 19. Specific HC emission without supercharging.

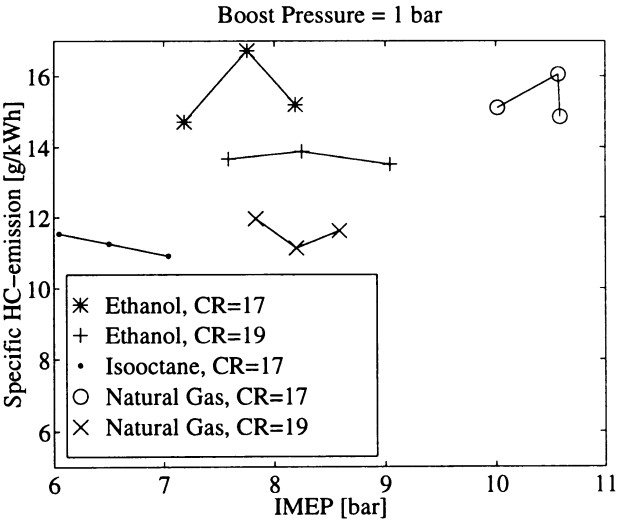

Figure 20. Specific HC emission for 1 bar boost pressure.

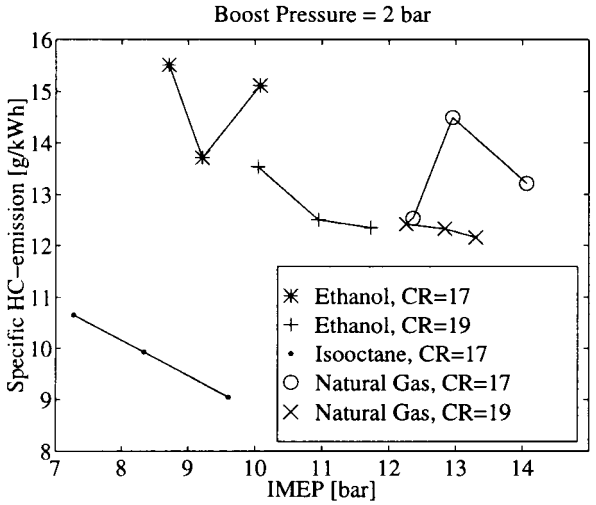

Figure 21. Specific HC emission for 2 bar boost pressure.

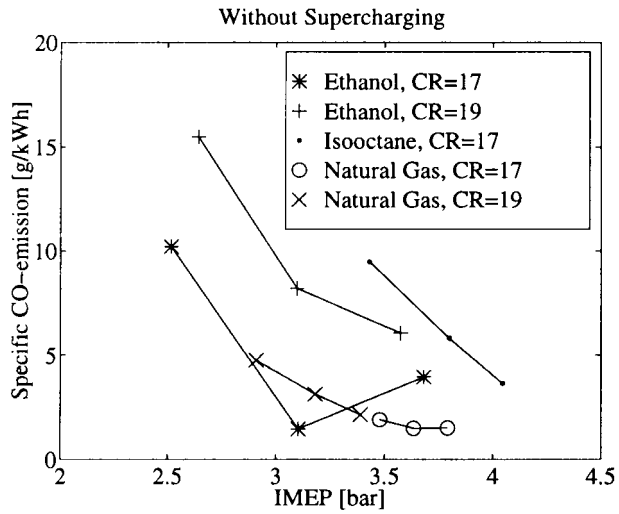

Figure 22. Specific CO emission without supercharging.

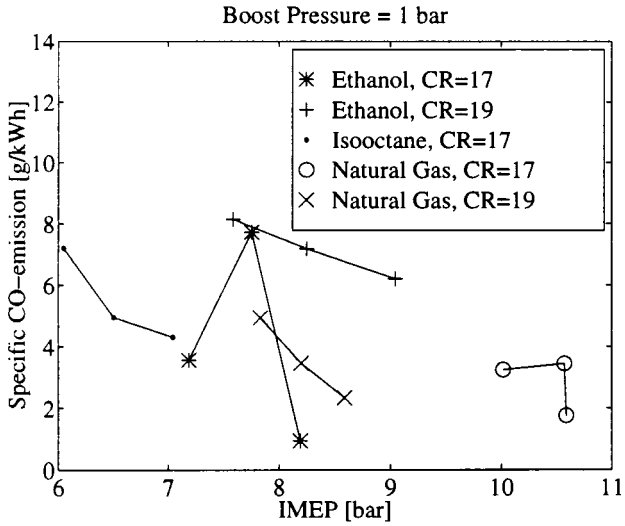

Figure 23. Specific CO emission for 1 bar boost pressure.

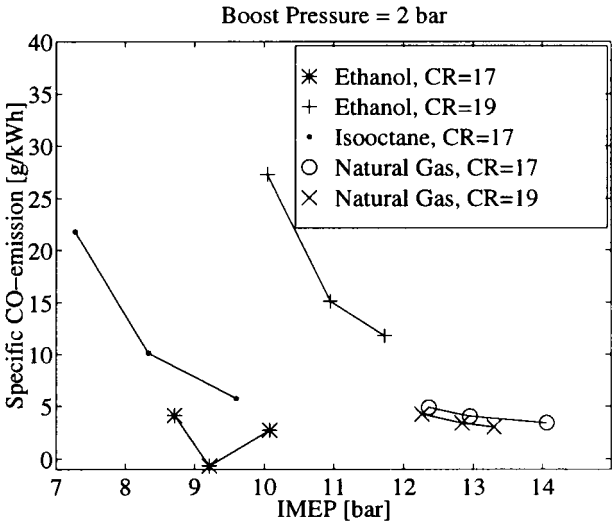

Figure 24. Specific CO emission for 2 bar boost pressure.

CYLINDER PRESSURE – The cylinder pressure was measured for all operating conditions. The cylinder pressure was recorded for 200 cycles, every 0.2 degrees crank angle. Figures 25-39 show the pressure trace. For all plots, the trace with the highest maximum pressure corresponds to the operating condition with the richest mixture, as given by Figures 1-3, and the lowest maximum pressure corresponds to the leanest case. The maximum rate of pressure rise was evaluated from the mean pressure trace using 200 cycles. Close to the stability limit of combustion, the crank angle position for combustion can fluctuate somewhat. This means that the value given can be underestimated. Even so, the rate of pressure rise, as given, is very high. The noise limit for SI operation at part load is around 4 bar/CAD, and the stress limit for large diesel engines is 6-10 bar/CAD. However, our converted diesel engine has been running with over 40 bar/CAD for short periods and at 15-20 bar/CAD for extended time periods without any sign of wear.

The maximum pressure obtained during the cycle with 2 bar of boost pressure is also of considerable magnitude. But as for the pressure rise rate, the base engine used can handle the stress without any problems. However, it is not advisable use a spark plug for combustion initiation when running at these pressures. The mechanical stress limit for the plug can be reached with serious consequences.

RATE OF COMBUSTION – The cylinder pressure was analysed using a single zone heat release model, which gave the rate of heat release. Details concerning the model can be found in [14]. Figures 25-39 also show the rate of heat release. The start of combustion is sensitive to the temperature history during the compression stroke. The runs shown in Figures 25-39 are all with the inlet temperature adjusted to get a reasonable combustion phasing. A few data sets have an inlet temperature which gives a combustion phase slightly early in the cycle. Those are *iso*-octane with boost pressure of 1 and 2 bar and ethanol with CR=17 and 2 bar of boost. The early phasing also results in reduced efficiency as shown in Figures 4-6. The reason for running these data sets with an early combustion is stability. With combustion at TDC or even after TDC, the limit for autoignition is reach. Even a slight decrease in temperature will decrease the combustion rate. The reduced combustion rate will then will lead to cooling of the walls and give an even colder charge next cycle. If combustion is lost, the inlet temperature must be increased 20-30 K to restart combustion. The experiments were conducted without closed loop control of combustion and a safety margin was hence useful.

COMBUSTION DURATION – The duration of 10-90 % (main combustion) heat released is often a very good parameter to use in discussions on fast or slow combustion. Figures 40-42 show the duration between 10 and 90 % of the heat released. The combustion duration shows a strong dependence on air/fuel ratio with HCCI. Close to the rich limit, the combustion is very fast, and approaches the ideal cycle with all the heat released at TDC. Using a leaner mixture, combustion is only twice as fast as in a normal SI engine. For the supercharged cases, the combustion duration is longer than for the NA cases. This depends on that a greater amount of mixture should burn in the supercharged cases. Hence, if the duration of combustion is to be the same for a supercharged case as for a NA case, the rate of combustion must be higher for the supercharged case, for a given value of λ.

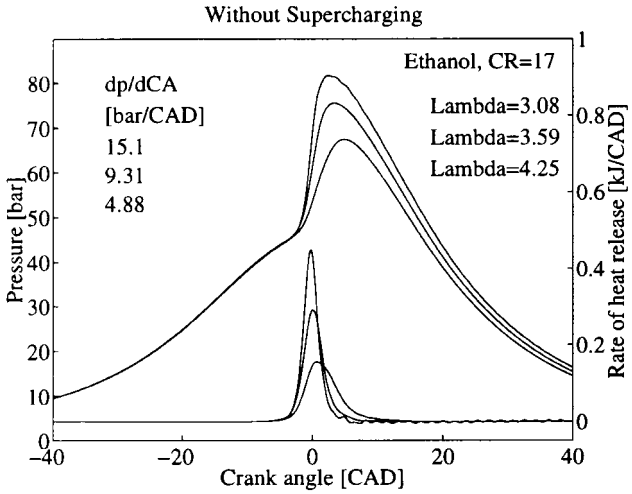

Figure 25. Cylinder pressure and rate of heat release without supercharging, running on ethanol with CR=17.

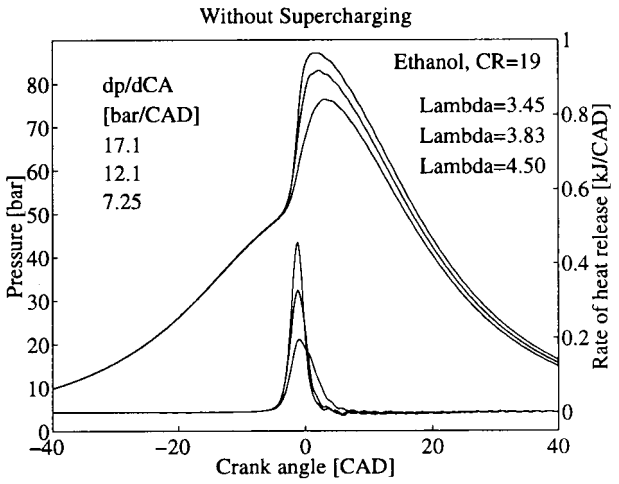

Figure 26. Cylinder pressure and rate of heat release without supercharging, running on ethanol with CR=19.

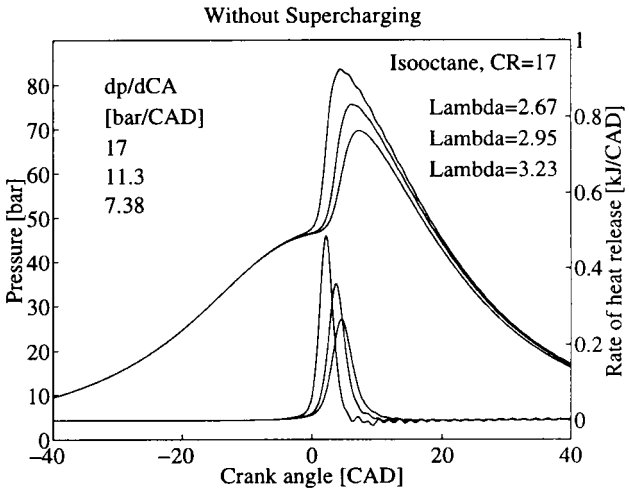

Figure 27. Cylinder pressure and rate of heat release without supercharging, running on iso-octane.

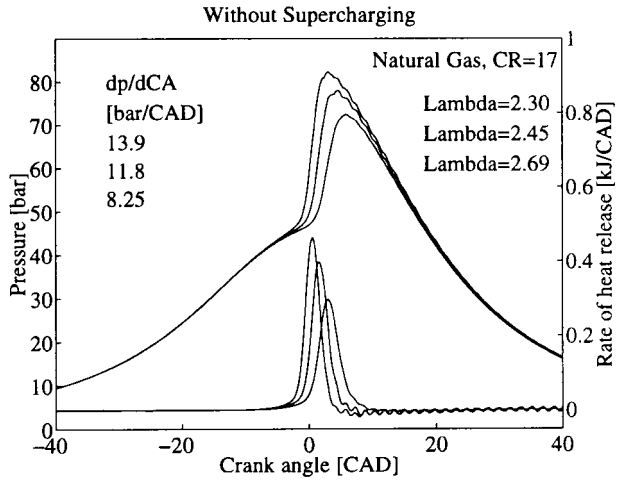

Figure 28. Cylinder pressure and rate of heat release without supercharging, running on natural gas with CR=17.

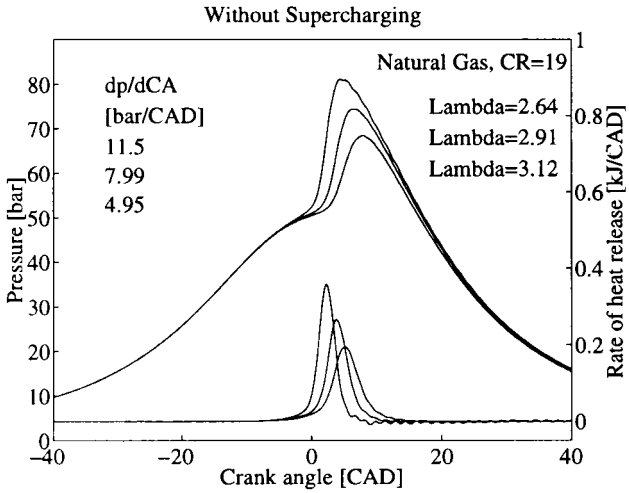

Figure 29. Cylinder pressure and rate of heat release without supercharging, running on natural gas with CR=19.

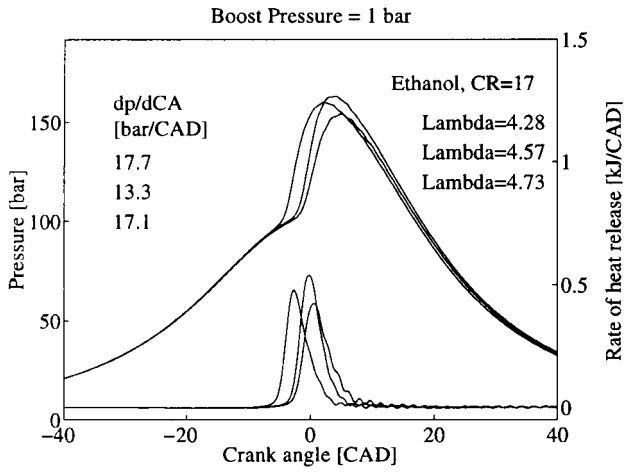

Figure 30. Cylinder pressure and rate of heat release with 1 bar boost pressure, running on ethanol with CR=17.

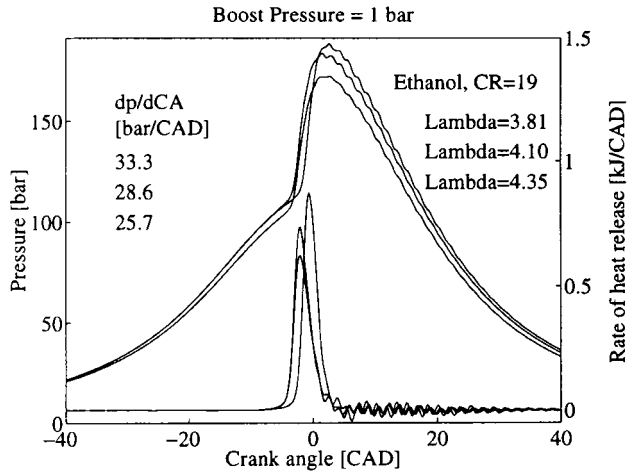

Figure 31. Cylinder pressure and rate of heat release with 1 bar boost pressure, running on ethanol with CR=19.

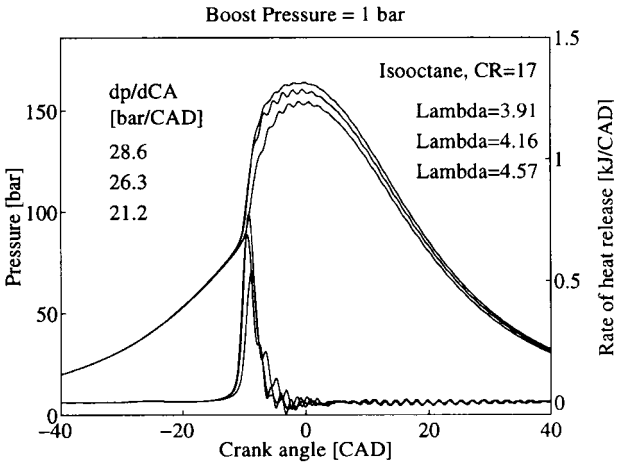

Figure 32. Cylinder pressure and rate of heat release with 1 bar of boost pressure, running on iso-octane.

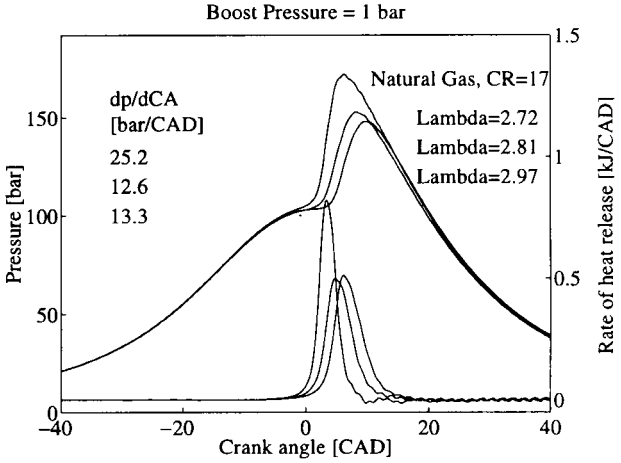

Figure 33. Cylinder pressure and rate of heat release with 1 bar boost pressure, running on natural gas with CR=17.

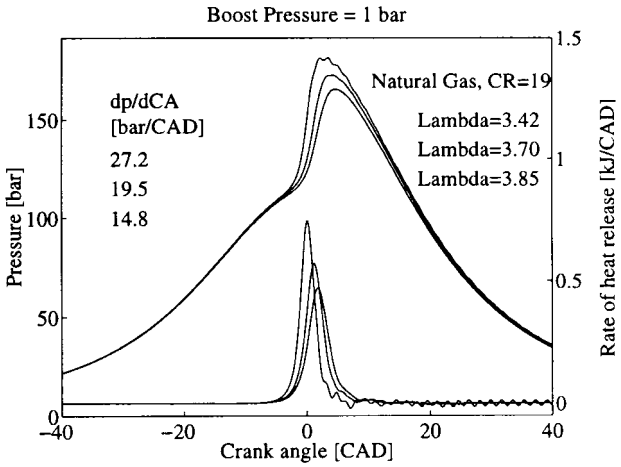

Figure 34. Cylinder pressure and rate of heat release with 1 bar boost pressure, running on natural gas with CR=19.

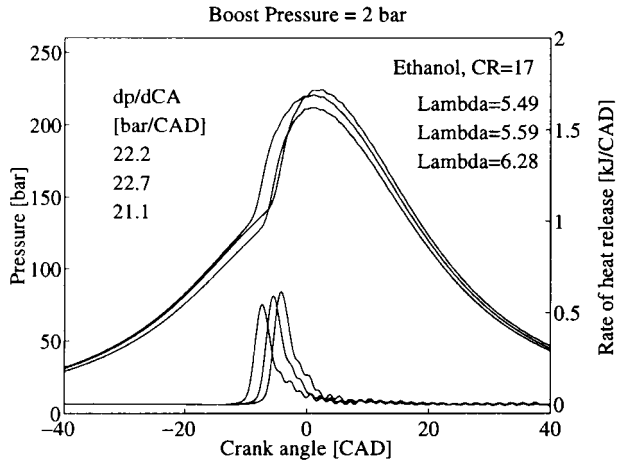

Figure 35. Cylinder pressure and rate of heat release with 2 bar boost pressure, running on ethanol with CR=17.

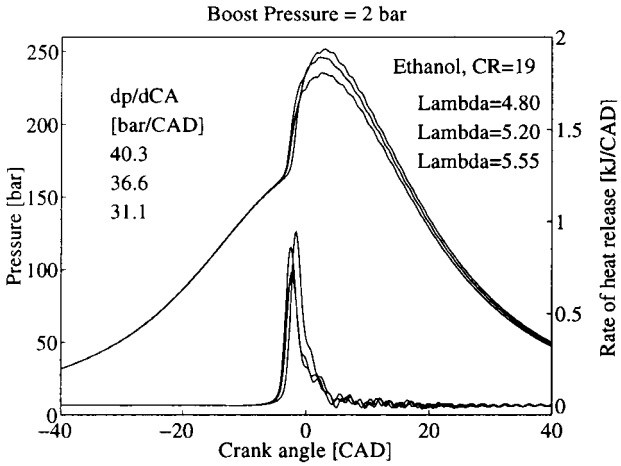

Figure 36. Cylinder pressure and rate of heat release with 2 bar boost pressure, running on ethanol with CR=19.

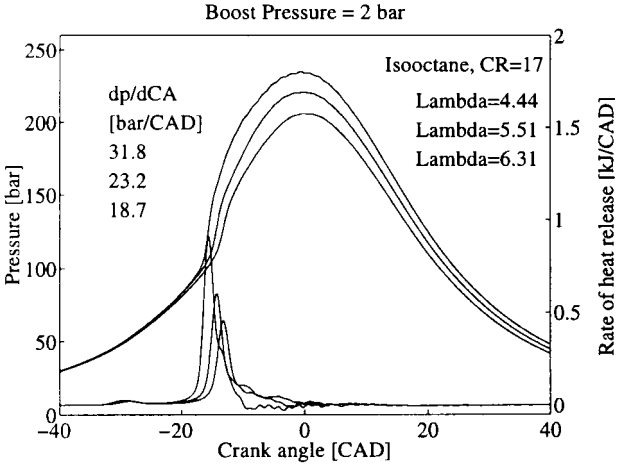

Figure 37. Cylinder pressure and rate of heat release with 2 bar boost pressure, running on iso-octane.

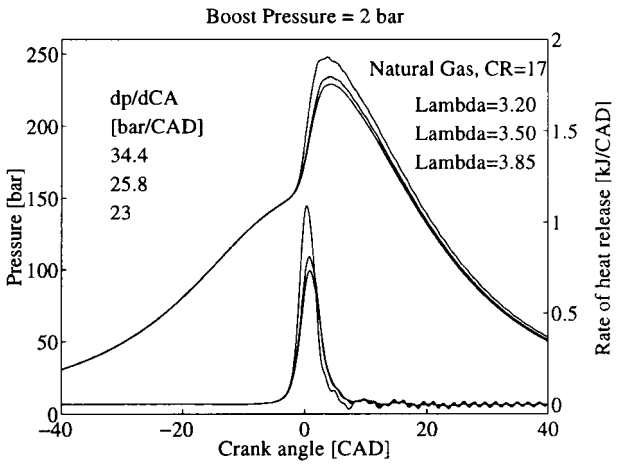

Figure 38. Cylinder pressure and rate of heat release with 2 bar boost pressure, running on natural gas with CR=17.

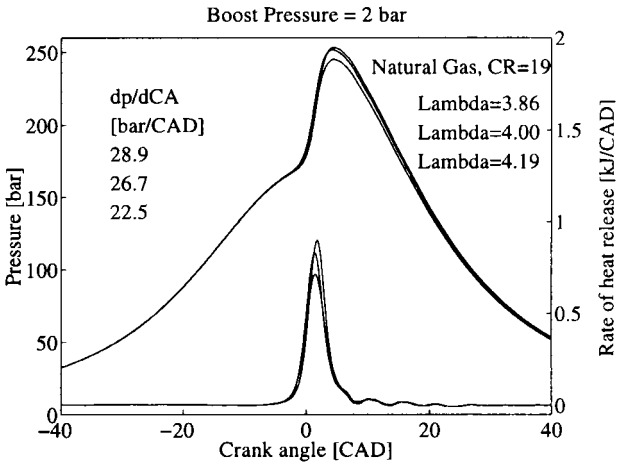

Figure 39. Cylinder pressure and rate of heat release with 2 bar boost pressure, running on natural gas with CR=19.

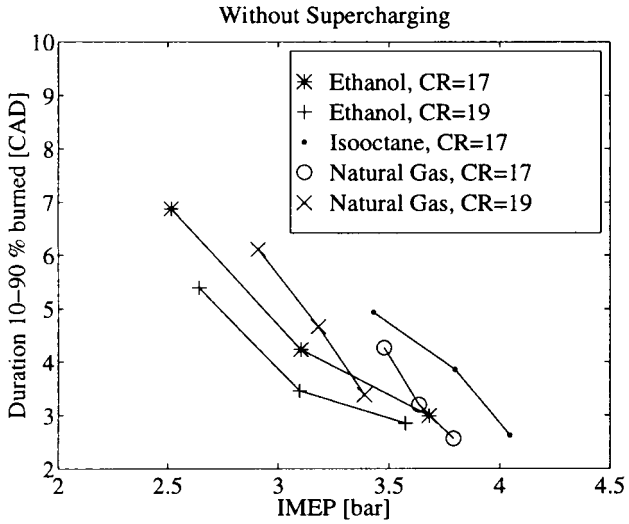

Figure 40. Combustion duration without supercharging.

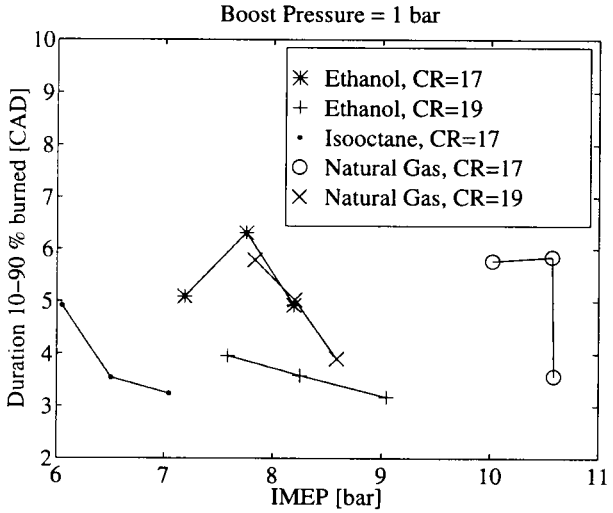

Figure 41. Combustion duration with 1 bar boost pressure.

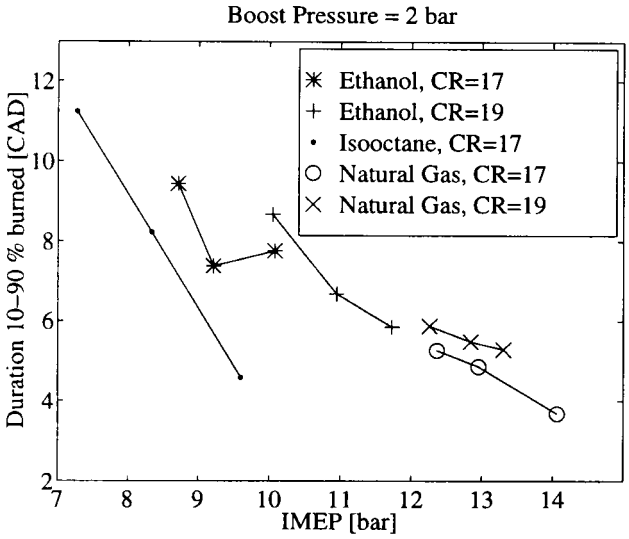

Figure 42. Combustion duration with 2 bar boost pressure.

COMPUTER SIMULATIONS

MODEL – The computer program used to simulate the combustion process in the engine is basically a set of zero-dimensional, time dependent differential equations. The program uses a detailed kinetic reaction scheme [16], considering energy and mass conservation balance for each chemical species in the reaction scheme. The time dependent values of temperature, pressure and mean molecular weight, and the concentrations of the chemical species and radicals involved in the reactions can thus be calculated.

THE HCCI MODEL – The main characteristics of this computer program and some details have been presented previously [17][18]. The HCCI engine simulations, however, require some specific differences in calculation approach. The basic idea is that the pressure and the temperature are obtained from the experimental results at a specific crank angle position. The volume decrease,

and thus the pressure increase, due to the piston movement can easily be calculated. Thus, the total pressure is calculated as the sum of the inlet pressure, the pressure increase due to the piston movement, and the pressure increase due to chemical reactions. The conservation equation for the chemical species is given by:

$$\frac{dY_j}{dt} = \frac{M_j}{\rho}\sum_{k=1}^{N_r} \nu_{j,k}\omega_k \qquad \text{(Eq. 1)}$$

and the energy conservation equation is given by:

$$m\sum_{j=1}^{N_s}\left(\left(h_j - \frac{RT}{M_j}\right)\frac{M_j}{\rho}\sum_{k=1}^{N_r}\nu_{j,k}\omega_k\right) + p\frac{dV}{dt} + m(C_p - \frac{R}{M})\frac{dT}{dt} = 0 \qquad \text{(Eq. 2)}$$

The instantaneous volume is calculated following [19]:

$$V_{total} = V_c + \frac{\pi B^2}{4}(l + a - s) \qquad \text{(Eq. 3)}$$

where the distance between the crank angle axis and the piston pin axis, *s,* is obtained from:

$$s = a\cos\Theta + (l^2 - a^2\sin^2\Theta)^{1/2} \qquad \text{(Eq. 4)}$$

and clearance volume V_c, the bore diameter *B*, the connecting rod length *l* and the crank angle radius *a* are given by the engine geometry. The pressure is then calculated from the equation of state:

$$p = \rho\frac{RT}{M} \qquad \text{(Eq. 5)}$$

COMPARISON TO SHOCK TUBE EXPERIMENTS – The chemical kinetics was evaluated by comparison to some of the many shock tube experiments that have been carried out on methane oxidation [20][21][22]. The experiments were simulated with the constant volume approximation

$$p\frac{dV}{dt} = 0 \qquad \text{(Eq. 6)}$$

in equation (6). The correlation between calculated ignition delay times and experimental values is shown in Figure 58 for fuel/air equivalence ratios ϕ (=1/λ) between 0.2 and 5 and initial pressures between 1 and 5 bar. In [18] it was shown that the ignition delay time for all experiments could be expressed:

$$\tau[O_2]^{1.6}[CH_4]^{-0.4} = 7.65\times10^{-8}\exp\left(\frac{51.4}{RT}\right) \qquad \text{(Eq. 7)}$$

where the gas constant, *R,* is given in [kcal, mole, K]. It can be seen in Figure 43 that the calculated ignition delay times are longer than the experimental values.

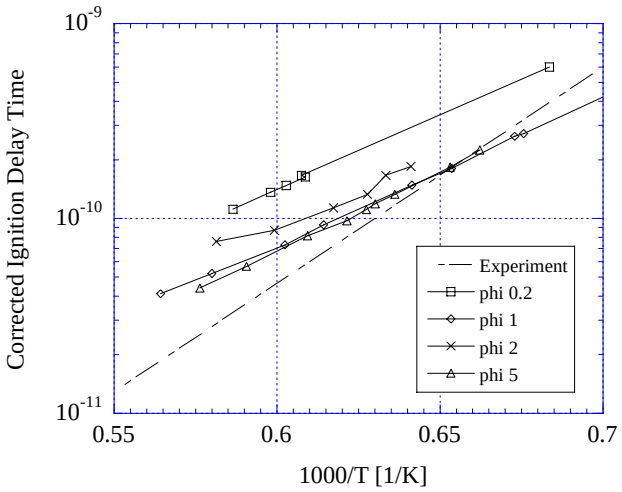

Figure 43. Calculated values of correlated ignition delay times for ϕ=0.2, 1, 2 and 5 respectively, compared with the relation (broken line) obtained from Seery and Bowman in [18].

COMPARISON WITH ENGINE EXPERIMENTS – Simulations have been made for two different levels of boost pressure, with three different fuel/air equivalence ratios for each boost pressure level. The initial temperature and initial pressure were obtained from the experiments (see table 3), using crank angle position 60 CAD BTDC as a starting point for the calculations.

Table 3. Inlet values for engine simulations

Case	Boost Pressure	ϕ	CR	T_{inlet}(K)	P_{inlet}(bar)
1	*1 bar*	*0.337*	*16.8*	*585*	*9.79*
2	*1 bar*	*0.356*	*16.8*	*582*	*9.89*
3	*1 bar*	*0.368*	*16.8*	*580*	*9.90*
4	*2 bar*	*0.261*	*16.6*	*592*	*14.3*
5	*2 bar*	*0.283*	*16.6*	*591*	*14.2*
6	*2 bar*	*0.310*	*16.6*	*590*	*14.2*

The calculated temperature and pressure are dependent on crank angle degree as shown in Figures 44 and 45. As already indicated by the shock tube experiments the calculated ignition delay times are longer than the experimental values. At the same time the calculated pressure rise is higher than values obtained from the experiments.

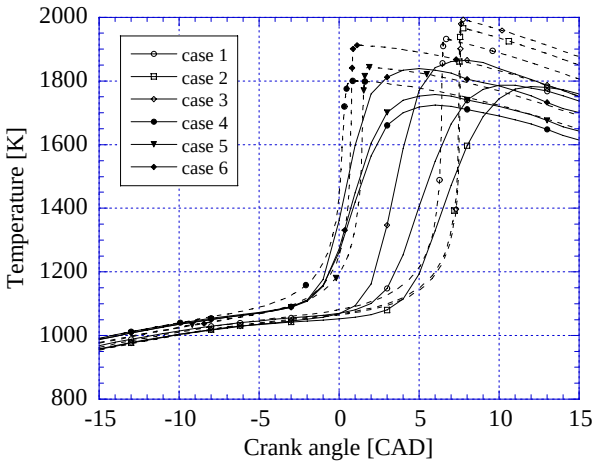

Figure 44. Comparison of measured temperature values and values obtained from the computer simulations when engine is supercharged at 1 and 2 bar boost pressure respectively. Dashed lines indicate simulated curves.

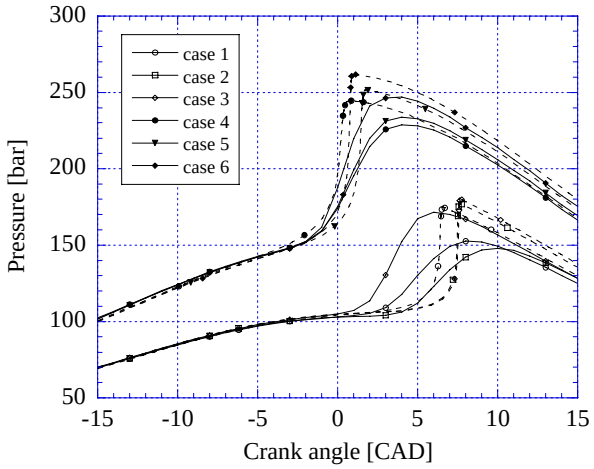

Figure 45. Comparison of measured pressure values and values obtained from the computer simulations when engine is supercharged at 1 and 2 bar boost pressure respectively. Dashed lines indicate simulated curves.

THE IGNITION-PROMOTING EFFECTS OF HIGHER HYDROCARBONS – The computer simulations suggest that the occurrence of some higher hydrocarbons, mainly ethane, propane and butane, in commercially available natural gas, may be of great importance in the autoignition process. An explanation [23] is that the thermal decomposition process of hydrocarbons generally starts with the abstraction of an H-atom. As a thermodynamic effect due to molecular orbital in hydrocarbons, a C-H-bond in a methane molecule is stronger than a C-H-bond in a primary bonded C-atom, which in turn, is stronger than a C-H-bond of a secondary bonded C-atom. As a result, a H-atom is likely to be abstracted from a butane molecule with two primary and two secondary H-atoms, less presumable to occur on an ethane molecule with only two primary C-atoms, and unlikely to be abstracted from a methane molecule.

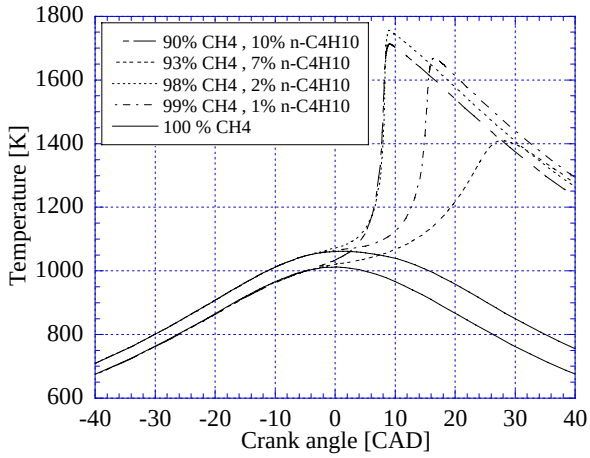

Figure 46. The effects of different amounts of butane in methane fuels. Calculation inlet values: CR=17, ϕ=0.25, P=15 bar at crank angle 60 CAD BTDC , and T=550 K and T=580 K at crank angle 60 CAD BTDC.

As shown in Figure 46, a small content (2 mole-% of the total gas fuel) of n-butane makes the HCCI process possible if the temperature is just below the autoignition level for pure methane fuel. On the other hand, if the temperature is 30 K lower, the n-butane content has to be increased substantially (10 mole-% of the total gas fuel) to achieve ignition with no change in ignition delay time.

DISCUSSION

The results presented show interesting characteristics of Supercharged Homogeneous Charge Compression Ignition. There are no combustion related problems in operating HCCI at high pressures. Up to two bar of boost pressure can be applied if the inlet temperature is adjusted accordingly.

The fuel used for HCCI should have a high octane number. This is indicated by the results obtained with *iso*-octane (100) which ignited early with high boost pressure, even with the lower compression ratio. Ethanol (106) could be operated at both 17:1 and 19:1, and showed the best efficiency. The fuel with the highest octane number, natural gas (120) gave the highest IMEP. This was due to the richer mixture and the relatively long ignition delay which caused combustion later during the exhaust stoke. As a consequence, the maximum pressure and pressure rise rate did not reach critical values as early as runs with *iso*-octane and ethanol.

The net indicated efficiency reported here is 59%. This very good efficiency must, however, be adjusted for the losses associated with friction and boost pressure supply. Two operating conditions can be used as examples. The first is the case with maximum net indicated efficiency, that is with ethanol, CR=19 with and an IMEP of 11 bar. If

we assume that the engine friction mean effective pressure, FMEP, is 1 bar and that the compressor delivering the boost pressure has an efficiency of 80% we obtain

$$\eta_b = \eta_{i,n}\frac{\text{IMEP} - \text{FMEP} - \text{BoostMEP}}{\text{IMEP}} = 0.59 \times \frac{11 - 1 - 2/0.8}{11} = 0.402$$

If we instead take the point with maximum IMEP, that is natural gas with 14 bar of IMEP we get

$$\eta_b = 0.53 \times \frac{14 - 1 - 2/0.8}{14} = 0.398$$

These examples show that the attainable brake efficiency is close to the values achieved in diesel engines. If the engine design is changed to reduce the considerable pumping losses, the brake efficiency could improved even more.

The major advantage with HCCI is, however, not the efficiency. It is instead the low exhaust emission levels of NO_X. At only a fraction of a ppm the NO_X level is below even the most stringent emission standards and this without the need of a sulphur-sensitive NO_X catalyst.

The emissions of HC and CO are ,however, not low. This means that exhaust aftertreatment must be used. Catalysts working in a lean environment to oxidize HC and CO are easy to find but as the exhaust gas temperature is extremely low special low-temperature catalysts would be required.

The simulations of the combustion process using chemical kinetics showed promising agreement with experiments. This suggests that computer programs using detailed chemical kinetics may in the future become a useful tool in designing HCCI-engines. Therefore, the detailed kinetic reaction scheme will be further developed to make it useable with alcohols and higher hydrocarbon fuels.

CONCLUSIONS

Supercharging dramatically increases the attainable IMEP for HCCI. The highest attainable IMEP was 14 bar using natural gas as fuel. This was achieved with 2 bar boost pressure and a compression ratio of 17:1, when the maximum pressure limit was set to 250 bar. With a lower compression ratio and higher boost pressure, an even higher IMEP would be possible to achieve, but at the price of lower efficiency.

The HC emission decreases with increasing boostpressure and engine load.

The CO emissions is very dependent on air/fuel ratio and preheating. Close to the rich limit and with hot inlet air, very little CO is generated.

Extremely little NO_X was generated in all cases. The values are as low as after a three-way catalyst or better.

REFERENCES

1. B. Johansson, H. Neij, M. Aldén, G. Juhlin: ”Investigations of the Influence of Mixture Preparation on Cyclic Variations in a SI-Engine, Using Laser Induced Fluorescence”, SAE950108
2. S: Onishi, S. Hong Jo, K. Shoda, P Do Jo, S. Kato: ”Active Thermo-Atmosphere Combustion (ATAC) - A New Combustion Process for Internal Combustion Engines”, SAE790501
3. M. Noguchi, Y. Tanaka, T. Tanaka, Y. Takeuchi: ”A Study on Gasoline Engine Combustion by Observation of Intermediate Reactive Products during Combustion”, SAE790840
4. N. Iida: ”Combustion Analysis of Methanol-Fueled Active Thermo-Atmosphere Combustion (ATAC) Engine Using a Spectroscopic Observation”” SAE940684
5. Y. Ishibashi, M. Asai: ”Improving the Exhaust Emissions of Two-Stroke Engines by Applying the Activated Radical Combustion”, SAE960742
6. Automotive Engineering, January issue 1997
7. P.Duret, S.Venturi: ”Automotive Calibration of the IAPAC Fluid Dynamically Controlled Two-Stroke Combustion Process”, SAE960363
8. P. Najt, D.E. Foster: ”Compression-Ignited Homogeneous Charge Combustion”, SAE830264
9. R.H. Thring: ”Homogeneous-Charge Compression-Ignition (HCCI) Engines”, SAE892068
10. T.W. Ryan, T.J. Callahan: ”Homogeneous Charge Compression Ignition of Diesel Fuel”, SAE961160
11. M. Stockinger,H. Schäpertöns,P.Kuhlmann: ”Versuche an einem gemischansugenden Verbrennungsmotor mit Selbstzündnung”, MTZ, Motertechnisches Zeitschrift 53 (1992) pp 80-85
12. M. Christensen, P. Einewall, B. Johansson: ”Homogeneous Charge Compression Ignition (HCCI) Using Iso-octane, Ethanol and Natural Gas- A Comparison to Spark Ignition Operation” SAE972874
13. T. Aoyama, Y. Hattori, J. Mizuta, Y. Sato: ”An Experimental Study on Premixed-Charge Compression Ignition Gasoline Engine”, SAE960081
14. B.Johansson: "On Cycle to Cycle Variations in Spark Ignition Engines", Ph.D. Thesis, ISRN LUTMDN/ TMVK-1010-SE, Dept. of Heat & Power Engineering, Lund Institute of Technology, Sweden
15. J.B. Heywood: ”Internal Combustion Engine Fundamentals” McGraw-Hill, New York, 1989
16. Chevalier C: ”Dissertation”, Universität Stuttgart 1993
17. S.Hajireza F. Mauss B.Sundén: ”Investigation of End-Gas Temperature and Pressure Increases in Gasoline Engines and Relevance for Knock Occurence”, SAE971671
18. J. Bood P-E Bengtsson F Mauss K Burgdorf I Denbratt: ”Knock in Spark-Ignition Engines: End-Gas Temperature Measurements Using Rotational CARS and Detailed Kinetic Calculations of the Autoignition process”, SAE971669
19. Heywood J B: “Internal Combustion Engines Fundamentals”, McGraw-Hill International Editions, 1989, ISBN 0-07-100499-8
20. D Seery C Bowman: ”An Experimental and Analytical Study of Methane Oxidation Behind Schock Waves”, Combust. Flame 14, pp 37-48

21. A Lifshitz K Scheller A Burcat G Skinner: ”Shock-Tube Investigation of Ignition in Methane-Oxygen-Argon Mixtures”, Combust. Flame 16, pp 311-321
22. E Petersen M Röhrig D Davidson R Hanson: ”High-Pressure Methane Oxidation Behind Reflected Shock Waves”, 26th Symposium (Int.) on Combustion, pp. 799-806, The Combustion Institute 1996
23. C Westbrook W Pitz W Leppard: ”The Autoignition Chemistry of Paraffinic Fuels and Pro-Knock and Anti-Knock Additives: A Detailed Chemical Kinetic Study”, SAE912314